Published in final edited form as:
Int J Cardiovasc Imaging. 2001 August ; 17(4): 287–296.

A comparison of prospective and retrospective respiratory navigator gating in 3D MR coronary angiography

Yiping P. Du[1], **Elliot R. McVeigh**[2], **David A. Bluemke**[3], **Harry A. Silber**[3], and **Thomas K.F. Foo**[1]

1*Applied Science Lab, GE-Medical Systems, Milwaukee, Wisconsin*

2*Department of Biomedical Engineering and Radiology, Johns Hopkins University School of Medicine, Baltimore, Maryland, USA*

3*Department of Radiology, Johns Hopkins University School of Medicine, Baltimore, Maryland, USA*

Abstract

A comparison between the prospective and retrospective respiratory navigator gating in MR coronary angiography was performed with eight normal subjects. A three-dimensional (3D) ECG-gated fast gradient echo pulse sequence was used for image data acquisition. The results show that the MR coronary angiography obtained using retrospective gating retains a considerable amount of motion artifacts. In this study, the images acquired using prospective navigator gating demonstrated significantly reduced motion artifacts ($p = 0.009$), improved vessel visibility ($p = 0.021$) with reduced imaging time ($p = 0.013$) compared to the images obtained using retrospective navigator gating.

Keywords

coronary imaging; MR imaging; MR navigator echoes

Introduction

MR coronary angiography is subject to cardiac and respiratory motion artifacts. Cardiac motion artifacts can be greatly reduced by using ECG gating. Respiratory motion can cause a substantial amount of ghosting in the images if it is not properly reduced or compensated. Two-dimensional (2D) ECG-gated MR coronary imaging can be completed within a breath-hold using fast imaging techniques [1,2]. The disadvantage of 2D MR coronary imaging is its low spatial resolution in the slice direction and possible misregistration of arteries in different slices [3,4]. Three-dimensional (3D) coronary imaging techniques, on the other hand, have the advantages of improved image signal-to-noise ratio and higher resolution in the slice-encoding direction. Furthermore, 3D image acquisitions are more suitable for imaging tortuous vessels as the resulting image data set can be reformatted in any arbitrary plane or curved line, or projected onto standard views of coronary angiography with volume rendering techniques. As implemented using current techniques, most 3D MR coronary angiography methods require several minutes to complete data acquisition. Because of the relatively longer scan time, 3D coronary imaging is prone to cardiac and respiratory motion artifacts. Great efforts have recently been made to acquire a 3D coronary image within a breath-hold [5]. This approach uses extra-vascular contrast agent for improved vessel contrast. More efforts, however, are

Address for correspondence: Yiping P. Du, PhD, Department of Radiology, University of Chicago, 5841 S. Maryland Avenue, MC 2026, Chicago, IL 60637, USA. Phone: (773) 834-4678; Fax: (773) 834-7610; E-mail: yipingdu@uchicago.edu.

needed before this approach is ready for routine clinical studies because it requires a fairly long breath-hold.

The navigator technique has been used to reduce respiratory motion artifacts in ECG-gated 3D MR coronary imaging [6]. In the navigator technique, a one-dimensional navigator echo is acquired to measure the displacement of the right hemi-diaphragm during scanning [7]. This displacement measurement is then used to determine whether or not the acquired imaging data should be retained for image reconstruction. Two approaches have been used to make such a determination: retrospective gating [8] and prospective gating [9]. In retrospective gating, the same location of the heart is over-sampled by a factor of 5, for instance, during breathing. A histogram of diaphragm displacement is then created using the navigator echo measurement for all the acquired echoes. The diaphragm position corresponding to the peak of the histogram is selected as the reference position. For each view, the echoes acquired at the diaphragm position that is the nearest to the reference position are retained for image reconstruction, and the remaining echoes are discarded.

Prospective gating has been used to reduce respiratory motion artifacts in 2D coronary imaging with spiral data acquisition [9]. In this approach, an accept/reject algorithm is used to reduce the respiratory motion artifacts. Using this approach, the image data acquisition is enabled when the diaphragm position is within a pre-determined window. The center of the window (or, the reference position) is usually located near end-expiration, where the diaphragm tends to be more stable and reproducible compared to other points in the respiratory cycle [10]. Prospective gating navigator was also implemented in rectilinear trajectories [11,12]. Compared to retrospective gating, prospective gating is more demanding of computational power of the scanner, because the MR scanner needs to process the navigator echo data before imaging data acquisition. A prospective accept/reject algorithm using navigator echoes has recently been implemented in a 3D fast gradient echo pulse sequence for coronary imaging [13]. Another variation of the prospective navigator algorithm, diminishing variance algorithm, has been developed by Sachs et al. [14] to progressively reduce motion artifacts during a scan. Studies have shown both retrospective and prospective gating techniques are very effective in reducing the respiratory motion artifacts in 3D coronary imaging [8,13,14]. However, a comparison between these two techniques has not yet been documented. In this paper, we report such comparison study with eight normal subjects.

Methods

Retrospective gating

In the retrospective gating studies, the data acquisition was similar to that used by Li et al. [8]. The 3D gradient-echo image data were acquired in eight normal male subjects using a 1.5 T SIGNA (GE-Medical Systems, Milwaukee, WI) equipped with an EchoSpeed gradient system (maximum gradient amplitude = 22 mT/m, maximum slew rate = 120 T/m/s). The ages of the eight subjects ranged from 22 to 43-years old, with the mean of 25.1-years old. A four-element cardiac phased array coil was used in all experiments. The imaging parameters were FOV = 28 × 21–32 × 24 cm^2, TR/TE/α = 6.5 ms/1.5ms/15°, matrix =256 × 192, 16 sections, slice thickness = 2 mm, readout bandwidth = 31.25 kHz. The k_z phase-encoding is along the anterior/posterior direction. The data along one k_y line were acquired in during one R–R period. In each of the k_y line, 16 echoes were acquired with z phase-encoding starting from $-k_z$ and ending at $+k_z$. A spectrally selective fat saturation pulse was applied immediately after the navigator pulse waveform and before the imaging pulse sequences. An ECG trigger delay, which is the time interval from the detection of the R wave to the start of the navigator echo, of 350–500 ms was used based on the heart rate of the subject. The delay from the R wave to the acquisition of the central echo (i.e., the echo with $k_z = 0$) was about 450–600 ms. The images

were zero-filled interpolated to a matrix size of 512 × 382 × 32 to reduce partial volume artifacts [15].

The data acquisition for the same slab was over-sampled by a factor of 5. The diaphragm position corresponding to each acquired phase encoding view was stored in a file for retrospective sorting. A histogram was calculated from the five data sets (5 × 192 points in total) of the diaphragm position. A diaphragm position corresponding to the peak of the histogram near the end-expiration was selected as the reference position. For each phase encoding view, the diaphragm position that was nearest to the reference position was considered as 'good'. In addition to these positions, the positions that were within 1 mm displacement from the reference position were also considered as 'good'. The 'good' echoes were then used to reconstruct the image. When there was more than one 'good' echo for a phase encoding view, the 'good' echoes were always averaged before image reconstruction in an attempt to improve the signal-to-noise ratio of the image [16].

In each of the experiments, we gave a brief coaching of breathing while the subject was on the table before moving into the magnet. In the coaching, we asked the subjects to relax and to have stable and shallow breathing during scan. We also suggested the subjects to relax at the end of expiration. There was no breath coaching during the scans.

Prospective gating

In the prospective gating studies, 3D image data were acquired at the same location with the same subjects and the same imaging parameters as in the retrospective gating studies. In five of the eight subjects, the prospective gating data were acquired immediately before the acquisition of the retrospective gating data. In the other three subjects, the prospective gating data were acquired after the retrospective gating data. The alternation of the data acquisition order between these two groups of subjects was intended to reduce the effect of the data acquisition order on the statistical analysis. In these prospective gating studies, an acceptance window of ±2 mm was used. In an RR interval, data acquisition was enabled if the measured diaphragm position was within the acceptance window. Otherwise, the data acquisition remained disabled. Prior to image acquisition, a navigator pre-scan was performed for a duration of 70 heart beats to determine the end-expiration position, and thus the acceptance window. This pre-scan was not needed for retrospective gating.

Image display

A localized maximum-intensity-projection (MIP) algorithm was developed to depict the entire vessel segments in a single 2D image. A set of points was manually selected on each of the vessel segments at different sections by the XV 3.10a software (written by John Bradley, Bryn Mawr, PA) on an SGI workstation (Silicon Graphics Inc., Mountain View, CA). The in-plane coordinates displayed with the XV software combined with the section number of each of the selected points are saved in a file as the 3D coordinates of the point. In this algorithm, the selected points on a single vessel segment were connected by straight lines. This piece-wise straight connected lines were used to represent the vessel segment. A curved surface was then defined by any two neighboring vessel segments. If there is only one vessel segment on one side of the image, as the right coronary artery (RCA) shown in Fig. 3, this vessel segment will be used to define a surface that consists straight lines along the anterior/posterior direction. In the MIP, the maximum intensity in a range of five pixels along the superior/inferior direction around the curved surfaces was used in the projection.

Observational comparison

Blinded observational comparisons between the retrospectively and prospectively gated images were performed by an experienced radiologist (DAB) and an experienced cardiologist

(HAS). The comparisons consist of the grading of respiratory motion artifacts and vessel visibility. In the grading of respiratory motion artifacts, the observation was focused on the severeness of image quality degradation caused by the ripple-like lines, that were caused by respiratory motion. In the grading of vessel visibility, the observation was focused on the sharpness and smoothness of the left main (LM). The comparison of respiratory motion artifacts and vessel visibility between the prospectively gated images (p) and the retrospectively gated images (R) were scored in a range of −2 to 2 (i.e., −2: R was considerably better than P; −1: R was marginally better than P; 0: no noticeable difference between P and R; 1: P was marginally better than R; 2: P was considerably better than R). The averaged score from the two observers was used to represent the relative image quality between the retrospective and prospective gated images.

Measurements of motion artifacts

The respiratory motion artifacts in different images was estimated by measuring the mean and standard deviation (SD) of image intensity in a region-of-interest outside the chest. Because the phase-encoding was applied along the anterior/posterior direction, respiratory motion generate ghosting outside the chest. Both mean and SD were expected to be higher in images with higher respiratory motion artifacts.

Statistical analysis

A Wilcoxon-Signed-Rank test was used to determine whether there was a significant difference between prospective and retrospective gating with regard to vessel visibility, motion artifacts, and imaging time.

Results and discussion

The results of the observational comparisons are listed in Table 1. In each of the observations, the difference between the scores given by the two observers was no larger than 1. These results show that prospective gating provided improved vessel visibility compared to retrospective gating ($p = 0.021$). These comparisons also show that prospective gating provided reduced motion artifacts ($p = 0.009$). During the prospectively gated scans of Subjects 2 and 5, the diaphragm position was drifted away from the acceptance window. During this time period, no views were accepted. We then manually adjusted the acceptance window slightly during the scan until the diaphragm position at the end of expiration was within the acceptance window and the views started to be accepted again. The shift of the acceptance window contributed to the increased motion artifacts in the prospectively gated image with Subject 2, in which the amount of shift was 4.3 mm. Image degradation caused by the shift of acceptance window appeared to be fairly small in Subject 5, partly because of small amount of shift (i.e., 2.1 mm) used.

Two pairs of images at the location of LM obtained with retrospective gating and prospective gating from two subjects are shown in Figure 1. In the top row of Figure 1, the image acquired from a subject with prospective gating (top right) had considerably reduced respiratory motion artifacts and improved vessel visibility compared to the images obtained using retrospective gating (top left). In another subject, the images obtained from the retrospective (bottom left) and prospective gating (bottom right) have comparable respiratory motion artifacts and vessel visibility.

The measurements of the mean and SD of image intensity in a region-of-interest outside of the body are listed in Table 1. These measurements indicate that the images acquired with prospective gating had reduced respiratory motion artifacts compared to the images obtained using the retrospective gating ($p = 0.009$ for both mean and SD measurements).

The width of a diaphragm displacement histogram is another indication of the level of motion artifacts in the image. The full-width (FW), which represents the difference between the maximum and minimum displacements in the histogram, and full-width at half maximum (FWHM) of the prospectively and retrospectively gated histograms are shown in Table 1. In some of the cases when the histogram does not have a bell-shaped profile, we assigned FWHM with the same value of FW. The FW can be considerably larger in the retrospectively gated histograms than in the prospectively gated histograms, although the FWHM was generally smaller in the retrospectively gated histograms. A large FW of a histogram indicates that some of the views with large diaphragm displacement were used in the image reconstruction and, therefore, large respiratory motion artifact can be induced by these views. In Subjects 2 and 5, the FW were larger than 4 mm in the prospectively gated histogram. In these two scans, the edge of the diaphragm apparently drifted outside the acceptance window. The operator had to manually shift the acceptance window accordingly in order to continue the scan.

Imaging time is another figure of merit in the comparison of the prospective and retrospective gating approaches. Respiratory motion artifacts can be reduced by using longer imaging time. It can be achieved either by narrowing the acceptance window in prospective gating, or by over-sampling more data in retrospective gating. In the studies presented in this paper, the imaging time using prospective gating, including the pre-scan with 70 heart beats, and the imaging time using the retrospective gating are shown in Table 1. In seven out of eight subjects, the imaging time was shorter in prospective gating. In these eight subjects, the average imaging time was 16% (i.e., 12.6 vs. 15.0 min) shorter using prospective gating than using retrospective gating ($p = 0.013$).

Figure 2 shows the sections acquired from Subject 1 using prospective gating. The sections near the origin of LM are shown in the top row of Figure 2. A set of axial sections near the origin of the RCA is shown in the bottom row of Figure 2. Figure 3 shows an image processed with the localized MIP algorithm using the same data as in Figure 2. In this figure, a much longer vessel segment was depicted than that in a section of the original image data. The origins of both the LM and RCA were displayed in the same figure, although they were located in different sections. The image discontinuity observed in this figure represents the projection of anatomies at different locations onto one single projection. Because the displacement in superior/inferior direction between the root of RCA and the root of LM, Figure 3 appears to have ‘split screen’ in the middle.

Figure 4 shows the histograms of diaphragm displacement before and after the retrospective gating from Subject 4. In this example, the width of the histogram was greatly reduced after the retrospective gating. It was noted, however, that some of the views (i.e., the ‘good’ views used for reconstructing the image) still had large displacement after retrospective gating. In this figure, the largest displacement of the ‘good’ views was 10.0 mm relative to the peak of the histogram after the retrospective gating. Many of the other ‘good’ views also had a displacement larger than 2 mm. When the ‘good’ views with large displacement were located at the center of the *k*-space, the resulting image can suffer severe respiratory motion artifacts. As a comparison, the displacement of different views acquired using prospective gating was always confined in a range of ±2 mm, except in the cases where the drift of diaphragm position is considerable during imaging data acquisition and the acceptance window needs to be adjusted accordingly. The smaller variation of diaphragm displacement in the prospectively gated data resulted in reduced respiratory motion artifacts compared to that in the images obtained using the retrospective gating. In Figure 4, there is only one ‘good’ view which has very large displacement. In this case, it is possible to replace this point with interpolation in image reconstruction. In some of other subjects, although not shown in this paper, there are many ‘good’ views with large displacement. Replacing these points with interpolation could cause artifacts in the reconstructed images.

Conclusion

Some of the MR coronary angiograms obtained using retrospective gating retained a considerable amount of respiratory motion artifacts. These motion artifacts are largely caused by the views with large diaphragm displacements after retrospective gating. Prospective gating is able to effectively remove the views with large diaphragm displacements. The images obtained using prospective navigator demonstrate significantly reduced respiratory motion artifacts, improved vessel visibility with reduced imaging time compared to the images obtained using retrospective gating.

Acknowledgements

Dr McVeigh is an Established Investigator of the American Heart Association.

References

1. Atkinson DJ, Edelman RR. Cineangiography of the heart in a single breath-hold with a segmented turboFLASH sequence. Radiology 1991;172:357–360. [PubMed: 1987592]
2. Edelman RR, Manning WJ, et al. Coronary arteries: breath-hold MR angiography. Radiology 1991;181:641–643. [PubMed: 1947074]
3. Wielopolski PA, Scharf JG, Edelman RR. Multislice coronary angiography within a single breath-hold. J Magn Reson Imaging 1994;4(suppl):80.
4. Hardy, CJ.; Dumoulin, CL.; Darrow, RD. MR angiography using a hybrid multislice technique with fat/muscle suppression and fluoroscopic localization. Proc ISMRM, 5th Annual Meeting; Vancouver. 1997. p. 440
5. Li, D.; Carr, J.; Shea, SM., et al. Improved 3D breath-hold volume-targeted imaging of coronary arteries with extra-vascular contrast agent. Proc ISMRM, 8th Annual Meeting; Denver. 2000. p. 1629
6. Wang Y, Grimm RC, Rossman PJ, et al. 3D coronary MR angiography in multiple breath-holds using a respiratory feedback monitor. Mag Reson Med 1995;34:11–16.
7. Wang Y, Riederer SJ, Ehman RL. Respiratory motion of the heart: kinematics and the implications for the spatial resolution in coronary imaging. Magn Reson Med 1995;33:713–719. [PubMed: 7596276]
8. Li D, Kaushikkar S, Haacke EM, et al. Coronary arteries: three-dimensional MR imaging with retrospective respiratory gating. Radiology 1996;201:857–863. [PubMed: 8939242]
9. Sachs TS, Meyer CH, Hu BS, et al. Real-time motion detection in spiral MRI using navigators. Magn Reson Med 1994;32:639–645. [PubMed: 7808265]
10. Taylor AM, Jhooti P, Wiesmann F, et al. MR navigator-Echo monitoring of temporal changes in diaphragm position: implications for coronary angiography. JMRI 1997;7:629–636. [PubMed: 9243380]
11. McConnell MV, Khasgiwala VC, Savord BJ, et al. Prospective adaptive navigator correction for breath-hold MR coronary angiograhpy. Magn Reson Med 1997;37:148–152. [PubMed: 8978644]
12. Oshinski JN, Hofland L, et al. Magnetic resonance coronary angiography using navigator echo gated real-time slice following. Int J Card Imaging 1998;14:191–199. [PubMed: 9813756]
13. Foo TKF, Ho VB, King KF. A computationally efficient method for tracking reference position displacement for motion compensation in magnetic resonance imaging. Magn Reson Med 1999;42:548–553. [PubMed: 10467299]
14. Sachs TS, Meyer CH, Irarrazabal P, et al. The Dimsinishing variance algorithm for real-time reduction of motion artifacts in MRI. Magn Reson Med 1995;34:412–422. [PubMed: 7500881]
15. Du YP, Parker DL, et al. Reduction of partial-volume artifacts with zero-filled interpolation in three-dimensional MR angiography. JMRI 1994;4:733–741. [PubMed: 7981519]
16. Li D, Paschal CB, et al. Coronary arteries: three-dimensional MR imaging with fat saturation and magnetization transfer contrast. Radiology 1993;187:401–406. [PubMed: 8475281]

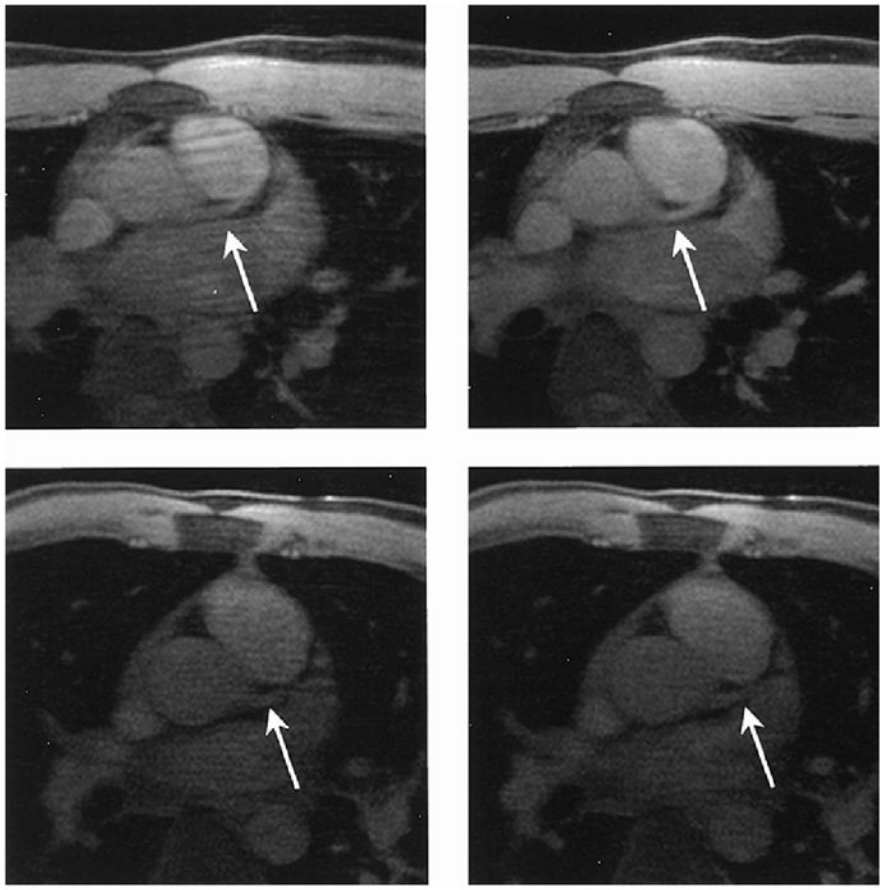

Figure 1.
Images acquired with retrospective gating (left) and prospective gating (right) in a section near the origin of the LM coronary artery from two subjects. In the top row, the image acquired with prospective gating (top right) had reduced respiratory motion artifacts and improved vessel visibility compared to the image acquired with retrospective gating (top left). In another subject, the images acquired with retrospective gating (bottom left) and prospective gating (bottom right) resulted in comparable respiratory motion artifacts and vessel visibility.

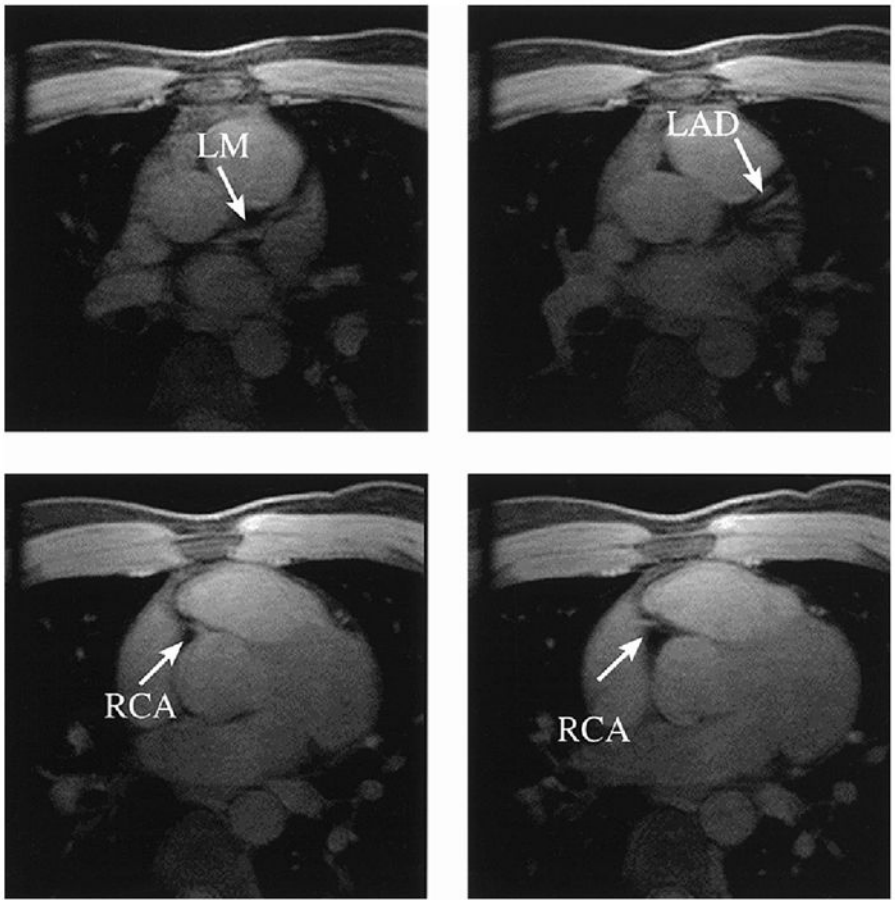

Figure 2.
A set of axial images from Subject 1 with prospective gating acquired at locations near the origin of the LM (top) and origin of the RCA (bottom).

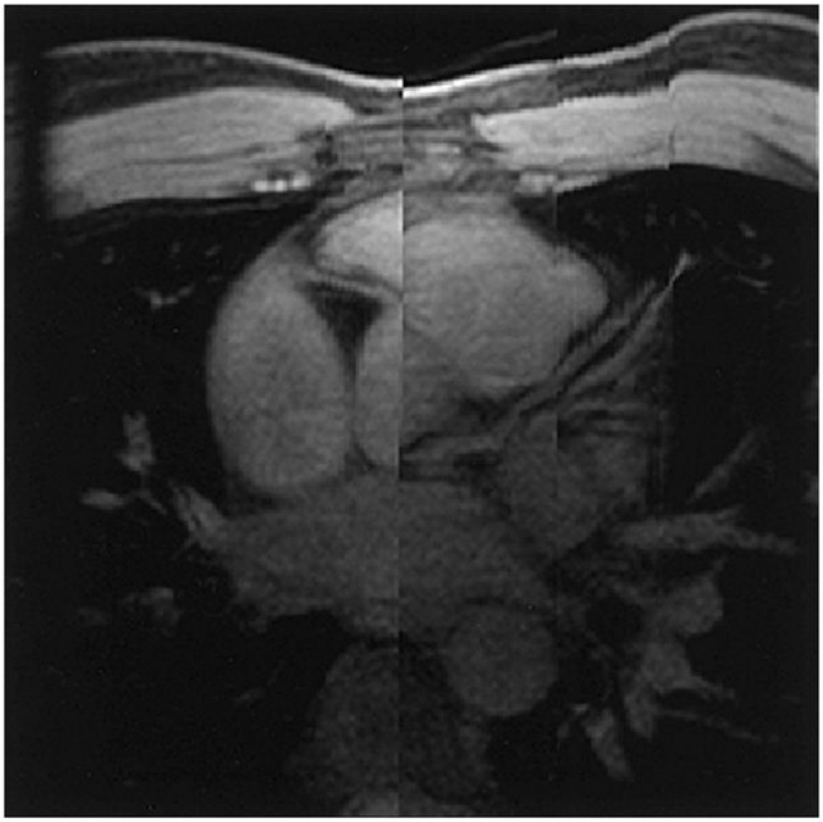

Figure 3.
An image processed with a localized MIP algorithm using the same 3D data set as shown in Figure 2. This figure shows much longer segments of the coronary arteries than the sections shown in Figure 2. Because the displacement in the superior/inferior direction between the root of RCA and the root of LM, this figure appears to have ‘split-screen’ in the middle.

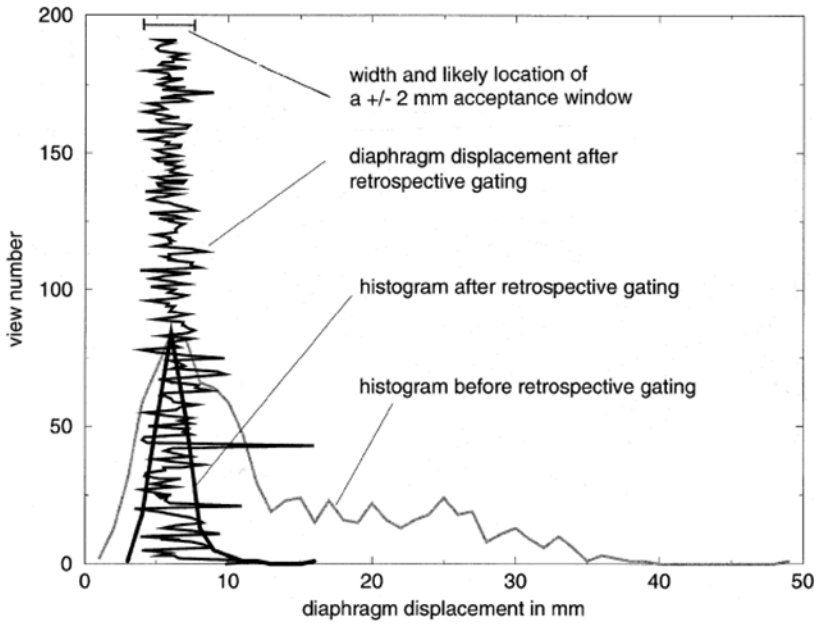

Figure 4.

The histograms of the diaphragm displacement before and after retrospective gating from Subject 4. The diaphragm displacement of each of the views using retrospective gating is also shown in this figure. The diaphragm displacement with retrospective gating can be as high as 10.0 mm relative to the peak of the histogram (at view number = 43). The views with a large diaphragm displacement after retrospective gating can cause considerable respiratory motion artifacts, especially when these views are located near the center of the *k*-space. In comparison, the diaphragm displacement with prospective gating is confined in the range of ±2 mm. In this figure, we also show the width and the likely location of the acceptance window if prospective gating were used during this part of the experiment.

Table 1

The observational and quantitative comparison between the prospective and retrospective gating approaches

Subject	Clinicians' observation		Intensity in air mean (SD)		Width of histogram (mm) (FWHM/FW)		Imaging time (mm)	
	Motion artifacts	Vessel visibility	Prospective	Retrospective	Prospective	Retrospective	Prospective	Retrospective
1	1.5	1.5	63.9 (18.3)	82.0 (28.3)	1.2/2.6	2.1/5.2	12.3	17.8
2	−0.5	0.5	155.6 (46.1)	168.4 (45.7)	7.4/8.3	1.8/18.4	11.1	15.0
3	1	1	72.3 (21.8)	80.6 (25.1)	1.4/2.2	1.6/16.4	12.0	14.0
4	2	2	112.6 (41.8)	117.2 (43.6)	1.9/4.0	2.6/12.4	15.0	14.1
5	2	2	104.6 (33.8)	159.0 (57.9)	1.4/6.1	2.0/38.4	12.0	13.2
6	1.5	1.5	68.7 (21.9)	69.7 (24.6)	3.9/3.9	2.4/13.5	15.3	18.1
7	2	0.5	114.7 (37.9)	119.2 (39.1)	3.0/3.6	2.0/13.2	11.2	15.0
8	1	−1	164.8 (49.6)	167.4 (51.6)	3.9/3.9	2.1/9.9	12.2	12.8
Average	1.31	1.0	107.2 (33.9)	120.4 (39.5)	3.0/4.3	2.1/15.9	12.6	15.0